3. Exploring *Macro* and *Micro* Level Connectivity of the Urea Phase in Slabstock Flexible Polyurethane Foam Formulations Using Lithium Chloride as a Probe

3.1 Chapter Summary

Urea phase connectivity has been probed by systematically varying the hard segment content, and lithium chloride content, in a series of plaques based on slabstock flexible polyurethane foams. The plaque formulations are identical to those of slabstock polyurethane foams with the exception that a surfactant is not utilized. SAXS is used to demonstrate that all materials investigated are microphase separated with similar interdomain spacings, irrespective of hard segment content (21 – 37 wt%) or LiCl content. Several complimentary characterization techniques are employed to reveal that urea phase connectivity is present at different length scales. *Macro* level connectivity, or connectivity of the large-scale urea rich aggregates typically observed in flexible slabstock polyurethane foams, is probed using SAXS, TEM, and AFM. These techniques collectively show that the urea aggregation increases as the hard segment content is increased. Incorporation of LiCl is shown to systematically reduce the urea aggregation behavior, thus leading to a loss in the *macro* connectivity of the urea phase. WAXS is used to probe the regularity in segmental packing, or the *micro* level connectivity between the hard segments, which is observed to decrease systematically on addition of LiCl. The loss in *micro* level connectivity is suggested to increase chain slippage, and leads to increased rates of stress-relaxation for the samples containing LiCl. Materials containing LiCl also display relatively short rubbery plateaus as compared to their counterparts which do not contain the additive. Modulus values, as obtained at ambient conditions by stress-strain analyses, are found to be a stronger function of LiCl content when the hard segment content is higher.

3.2 Introduction

Polyurethanes, hereafter abbreviated as PU in this chapter, are utilized in a variety of applications such as foams, elastomers, adhesives, coatings, and sealants [1]. These materials have interested a broad spectrum of scientists with respect to their chemistry and physical properties. By volume, the use of polyurethanes as flexible foams accounts for more than 50% of

the total PU production [2]. Flexible PU foams, which are available in a wide range of softness or firmness, resilience, and density; are primarily used in the transportation, furnishing, and packaging industries.

Flexible PU foams are produced by catalytically balancing two well understood reaction schemes. In the first reaction, called the 'blow' reaction, an isocyanate group reacts with water to yield an amine functionality, carbon dioxide, and heat. The amine formed further reacts with another isocyanate group to yield a urea linkage. The carbon dioxide generated in this exothermic reaction helps to expand the already nucleated bubbles in the reaction mixture into foam cells. Since the isocyanates utilized are usually difunctional, further reaction with water leads to chain extension by which urea hard segments are generated. In the second reaction, known as the 'gelation' reaction, an isocyanate group reacts with a hydroxyl group (usually from a trifunctional polyol) to form a urethane linkage. This reaction covalently bonds the urea hard segments to the flexible polyol chains.

Microphase separation occurs when the concentration of the urea hard segments surpasses a system-dependent solubility limit, leading to the formation of urea microdomains. These microdomains achieve their cohesive strength from strong hydrogen bonding interactions. In addition, they serve to enhance the stiffness of the foam by acting as physical cross-linking points, and by causing a filler-like effect. The polyols used have an average functionality in the range of 2.5-3, and thus provide the covalent cross-linking points.

Workers have observed in foams with relatively high water content (and therefore higher hard segment content) the presence of larger scale structures which are not completely understood [3,4]. Large precipitates of urea rich phases, also referred to as 'urea balls' or 'urea aggregates' have been observed via TEM [2,3] and x-ray microscopy (XRM) [4] although there is limited knowledge regarding the exact nature of formation, as well as the detailed composition of these aggregates. The aggregates size has been estimated to be ca. 0.3 μm in typical slabstock foams [3]. Also, it has been noted that the presence of urea rich aggregates is substantially reduced in molded foams [2]. These differences in the urea aggregation behavior arise due to differences in the foam components used in slabstock and molded foams. Although both kinds of foams typically utilize the 80:20 2,4/2,6 TDI isomer mixture, they differ considerably in other formulation components. The polyols utilized in molded foams are generally higher molecular weight (ca. 5000 g/mol as compared to ca. 3000 g/mol for slabstock foam polyols), have higher

ethylene oxide (EO) contents, and are also usually EO end-capped. This leads to molded foams achieving a faster viscosity build-up and enhanced reaction rates, both of which are necessary to ensure shorter demold times. The presence of higher EO contents in molded foams promotes solubility of the different phases involved which is thought to reduce the urea phase aggregation. Molded foam formulations often employ a copolymer polyol (CPP) which acts as a particulate filler and improves the load bearing properties of the foam [5]. Also, since the urea aggregation is minimized in molded foams, this suppresses one of the cell-opening mechanisms. The presence of a copolymer polyol serves as an additional mechanism to induce cell-opening [2].

Since shorter demold times are essential in molded foam processing, the formulations for this class of foams also involve the addition of a cross-linking agent [2]. The cross-linking agent which has gained commercial importance is diethanol amine (DEOA) and is added at levels of ca. 1.0 – 2.0 parts per hundred polyol (pphp). The influence of DEOA on structure-property relationships of molded flexible foams has been investigated [6,7,8]. Kaushiva and Wilkes [6] found that addition of DEOA altered the connectivity of the urea phase at different length scales. Using WAXS and FTIR they demonstrated that there was a loss in the bidentate hydrogen bonding of the urea hard segments on addition of DEOA. They suggested that DEOA primarily resided in the urea microdomains and reduced the regularity in segmental packing of the hard segments, leading to a loss in connectivity at the *micro* level. Using high magnification AFM images, the authors also demonstrated that there was the presence of ca. 50 nm size urea rich regions in foams which did not contain DEOA [9]. The addition of DEOA also suppressed the formation of these urea rich regions and instead ca. 5 nm sized urea microdomains were observed [9]. These changes in the morphology brought about notable changes in the mechanical properties. Foams containing DEOA exhibited lower rubbery moduli and lower load-bearing properties [6], thus suggesting that the connectivity of the urea phase played an important role in determining the physical properties of PU foams.

The importance of hydrogen bonding in determining the physical properties of flexible PU foams has been demonstrated in several other studies as well. Moreland et. al. extensively studied the viscoelastic behavior of slabstock foams under varied temperature and humidity conditions [10,11], and found that on increasing the relative humidity, water acted as a hard domain plasticizer and resulted in an increase in creep. They also reported that at higher relative humidity conditions, the creep rate was higher for higher hard segment containing foams, while

maintaining the same initial deformation level and testing conditions. This difference in creep rates was attributed to the greater amount of hydrogen bonds available for disruption in the higher hard segment containing foams. The mechano-sorptive behavior of flexible PU foams undergoing a creep experiment was investigated by Dounis et. al. [12]. In their experiment, foams were subjected to cyclic humidity conditions between 10 and 98%. It was shown that the compressive strain increased in subsequent steps, *with larger deformations observed during the desorption portion of the humidity cycling*. This somewhat surprising behavior was explained by suggesting that during the dehumidification process, there were regions of free volume introduced within the urea microdomains, which promoted chain slippage and the observed increases in strain. This study also enforced the importance of hydrogen bonding to physical properties of PU foams.

From the above discussion it is clear that hydrogen bonding of the urea hard segments plays a critical role in determining the mechanical and related properties of flexible PU foams. Therefore, in order to gain a better understanding of these materials, it would be desirable to use an additive in the foam formulation that leads to a disruption in the hydrogen bonding characteristics. The addition of such an additive in a systematic manner would serve as a means to alter the phase separation characteristics of PU foams and would give insight into urea phase connectivity. Lithium salts have been shown to disrupt hydrogen bonding in polymers. For this reason, lithium salts have been used for dissolution of polymer samples (for example, Kevlar) to measure their molecular weight distribution using gel permeation chromatography [13].

An examination of the orientation-elongation behavior of linear PU elastomers by Seymour et. al. [14] revealed that at low deformation, the hard segments oriented transverse to the stretching direction. At higher deformation levels, hard segment orientation parallel to the stretching direction was observed. This behavior was explained by suggesting that the hard segments formed lamellae-like structures which at low deformation levels oriented with their long axis parallel to the stretch direction. At higher deformation levels the lamellae-like structures were thought to rupture and hard segment orientation parallel to the stretching direction was observed. Similar conclusions were drawn by Moreland et. al. [15] who used linear IR-dichroism, and also by Kaushiva et. al. [16] who used WAXS to investigate the orientation-elongation behavior of the hard segments within slabstock PU foams. These studies further reinforce the idea that in PU foams the urea microdomains are not present as separate entities,

but at least some of them possess microdomain continuity leading to the formation of the proposed lamellae-like structures. Since the applications of PU foams often require them to be subjected to mechanical deformation, studies which can elucidate the nature of urea phase connectivity would be instrumental in further understanding their structure-property correlations.

Yontz et. al. analyzed the hard segment length distribution as a function of water content in a series of flexible PU foams using matrix-assisted laser desorption ionization (MALDI) mass spectroscopy [17]. The workers observed that on varying the water content between 3.5 and 7.5 pphp, hard segments with five urea repeat units predominated. Also, it was noted that increasing the water content promoted the formation of longer hard segments. While stoichiometry dictates an average of 4-6 repeating units in a hard segment, workers detected hard segments containing as high as 14 repeating units. The fraction of the longer hard segments was found to increase with the water content. These observations further suggest that hard segment connectivity might be promoted due to the presence of relatively longer hard segments in high hard segment content PU foams.

Moreland et. al. studied the effect of LiCl on slabstock PU foams in an attempt to produce lower modulus foams which maintained high hard segment contents and thereby required no auxiliary blowing agents [18]. They observed via SAXS and TEM that incorporation of LiCl led to the urea microdomains getting more homogeneously distributed in the soft polyol matrix. In that study, foams were prepared with 0.0, 0.4, and 0.5 LiCl pphp, while maintaining a constant hard segment content. It was suggested that LiCl acted as a local ‘hard segment plasticizer’, and systematically reduced the modulus of the foam with its increasing content. The present study, however, will focus on the use of this additive to probe urea phase connectivity and its influence on physical properties, and thus a broader range of LiCl contents, from 0.0 to 1.0 LiCl pphp has been investigated.

In light of the above discussion, it is clear that PU foams can possess vastly different morphologies with different levels of urea phase connectivity. Lithium chloride is an additive which does not covalently react into the polymer network, and yet leads to networks which possess different urea phase connectivity by changing the solubilization characteristics of the different phases involved, as well as by altering the reaction kinetics. It is also realized that materials with different hard segment contents would be expected to possess varied levels of urea phase connectivity based on volume fraction arguments. Therefore, the present work focuses on

varying not only the LiCl content, but also on studying the effect of hard segment content on urea phase connectivity and its influence on physical properties of plaques based on slabstock PU foams. Although there has been some debate on using plaques to investigate structure-property relationships of flexible PU foams [19], it has been shown that the *trends* observed in flexible PU foams are, in general, in good agreement with their plaque counterparts [3,10], which rationalizes the use of plaques to carry out the present study. The use of plaques also eliminates any complication which may arise due to the presence of a cellular structure, which affects the physical properties of an actual foam [2]. Chapter 4 will discuss the influence of LiCl on the other important class of *molded* flexible PU foams. In Chapter 5 it will be shown that LiCl is *not* a unique additive which can be used to probe urea phase connectivity, but other salts, such as LiBr can be utilized to achieve similar results. The influence of LiCl on *actual* flexible PU foams will be discussed in Chapter 6 which will also elucidate the interaction of LiCl at the molecular level with urea, urethane, and ether linkages.

3.3 Experimental

3.3.1 Materials

To examine urea phase connectivity in slabstock systems, plaques based on Voranol 3137® were prepared. Voranol 3137® is a 13% EO heterofed polyol with a 3000 molecular weight, and an average functionality of ca. 2.79. All formulations were based on the 80:20 2,4/2,6 TDI mixture, maintained at an index value of 100. The catalyst package used was a 5:1 mixture (by weight) of Dabco 33LV and Dabco BL11 and was used at 0.2 pphp. Chemical details of the catalysts can be found elsewhere [2]. Three series of plaques with varied hard segment content were prepared by varying the amount of water added as 2.0, 3.5, and 4.5 pphp. These water levels correspond to wt% hard segment contents of 21.0, 32.4, and 37.0 respectively. For each series, the LiCl content was varied as 0.0, 0.1, 0.5, and 1.0 LiCl pphp. In addition to these samples, a plaque containing 1.0 water pphp and 0.0 LiCl pphp was made.

The plaques were prepared in a lab-scale cup-foaming setup at Dow Chemical, Texas. The first step was to dissolve known amounts of LiCl in deionized water. Weighed amounts of polyol and aqueous LiCl were added to a 400 ml cup and stirred at 2000 rpm with a 1” diameter stirrer for 25 seconds. This was followed by the addition of TDI and the catalyst, and the mixture was stirred for another 15 seconds at the same stirring speed. Foam formation was suppressed by

forcing the foam to collapse by vigorous stirring. Just prior to gelation, the reacting mixture was quickly poured from the cup onto Teflon sheets which were supported by steel plates. A picture-frame mold ca. 0.05" thick was utilized. The compression of the plaque was carried out in a hot-press operating at 100 °C and 20,000 lb_f for 1 hour. At the end of 1 hour, the plaque was cut out from the picture-frame and allowed to cool at ambient conditions. It is acknowledged that the temperature of actual slabstock flexible PU foams exceeds 100 °C and it takes the large foam buns produced by this process a period of 24 hours to a few days to cool to room temperature. Also, no surfactant has been utilized to prepare the plaques since stabilization of the cellular structure is not required. Based on the above differences pointed out between the preparation of

Sample	TDI Index	Moles of TDI	Polyol (g)	Moles of Polyol	Water (g)	Moles of Water	LiCl (g)	Moles of LiCl
P1.0-LC0.0	100	0.102	100	0.033	1.0	0.055	0.0	0.000
P2.0-LC0.0	100	0.158	100	0.033	2.0	0.111	0.0	0.000
P2.0-LC0.1	100	0.158	100	0.033	2.0	0.111	0.1	2.3×10^{-3}
P2.0-LC0.5	100	0.158	100	0.033	2.0	0.111	0.5	11.7×10^{-3}
P2.0-LC1.0	100	0.158	100	0.033	2.0	0.111	1.0	23.5×10^{-3}
P3.5-LC0.0	100	0.241	100	0.033	3.5	0.194	0.0	0.000
P3.5-LC0.1	100	0.241	100	0.033	3.5	0.194	0.1	2.3×10^{-3}
P3.5-LC0.5	100	0.241	100	0.033	3.5	0.194	0.5	11.7×10^{-3}
P3.5-LC1.0	100	0.241	100	0.033	3.5	0.194	1.0	23.5×10^{-3}
P4.5-LC0.0	100	0.296	100	0.033	4.5	0.250	0.0	0.000
P4.5-LC0.1	100	0.296	100	0.033	4.5	0.250	0.1	2.3×10^{-3}
P4.5-LC0.5	100	0.296	100	0.033	4.5	0.250	0.5	11.7×10^{-3}
P4.5-LC1.0	100	0.296	100	0.033	4.5	0.250	1.0	23.5×10^{-3}

Table 3.1 – Formulations utilized for preparation of plaques

plaques and actual foams, one might expect marked differences in the morphologies of the resulting materials. This issue will be discussed in detail in Chapter 6. However, as mentioned earlier, plaques are known to display similar trends in structure-property correlations as compared to their foam counterparts [3,10], and this justifies their use to investigate PU foams.

Each sample is distinguished from other samples using a simple nomenclature scheme, as used in Table 3.1. As a reminder that 'plaques' based on foam formulations have been investigated, the first letter for all the samples in the nomenclature is 'P'. The 'P' is followed by

a number which indicates the water content. For example, 'P2.0' indicates a 2.0 water pphp plaque. This is followed by LC (for lithium chloride) and a number which describes the amount of LiCl added. For example, 'LC0.5' would indicate that the formulation contains 0.5 LiCl pphp.

3.3.2 Methods

Small angle X-ray scattering (SAXS) was utilized to study the presence of microphase separation and to follow trends in the urea aggregation behavior. This was done using a Philips model PW1729 generator operating at 40 kV and 20 mA. A slit collimated (0.03 x 5 mm^2) Kratky camera with nickel filtered CuKα radiation having a wavelength of 1.542 Å was used. The detector was a Braun OED 50 position-sensitive platinum wire detector. Raw data was corrected for parasitic scattering and normalized using a Lupolen standard.

To investigate the local ordering of the hard segments at the 1-10 Å level, wide angle x-ray scattering (WAXS) was employed. WAXS experiments were carried out using a Phillips model PW1720 generator equipped with a Warhus camera. Pinhole collimated (ca. 0.02 in. diameter), nickel filtered CuKα radiation with a wavelength of 1.542 Å was used. Plaque samples having a thickness of ca. 1.2 mm were exposed to x-rays for 5 hrs, with a sample to film distance of 5.5 cm.

The urea aggregation behavior was examined using TEM and tapping-mode AFM. Small enough areas of the plaques, which would be suitable for cryomicrotomy, were exposed by trimming away the surrounding regions using a razor blade. These exposed regions were cryogenically microtomed at ca. –90 °C using a Reichert Jung ultramicrotome Ultracut E equipped with a model FC-4D cryo-attachment. Ultra thin sections of the order of 80-100 nm were collected on 600 mesh copper grids using ethanol. Micrographs of the unstained samples were taken using a Philips 420T scanning transmission electron microscope (STEM) operating at an accelerating voltage of 100 kV.

Tapping-mode atomic force microscopy (AFM) was carried out to examine the urea aggregation behavior and also to follow trends in the relative 'hardness' of the urea phase as a function of LiCl content. Small samples were cut from the plaques and embedded in epoxy which was allowed to cure overnight at room temperature. The embedding was carried out to give the ca. 1.2 mm thin plaque enough rigidity to carry out the AFM experiment and to minimize vibrations. There was no interaction between the epoxy and the samples since the

samples were found to retain their original dimensions (no swelling) after embedding. The embedded samples were trimmed using a razor blade to expose small trapezoidal regions for microtoming. The trapezoidal regions were cryogenically microtomed in a manner similar to that used for TEM. AFM experiments were run using a Digital Instruments scanning probe microscope equipped with a Nanoscope IIIa controller. Nanosensors TESP (Tapping Etched Silicon Probe) single beam cantilevers with tip radii of 5-10 nm were utilized. The cantilevers had nominal lengths of 125 μm, force constants in the range of 35 ± 7 N/m, and were used at their resonant frequencies which ranged from 260-320 kHz. Both 'height' as well as 'phase' images were collected. The phase images were not influenced by variations in surface features and were thus dependent only on variations in the 'hardness' or 'softness' of the different phases. Therefore, only the phase images are presented in this report.

Differential scanning calorimetery (DSC) experiments were carried out to observe any changes in the soft segment T_g position as well as breadth on addition of LiCl. These experiments were conducted using a Seiko DSC 220C under a nitrogen purge. The heating rate was set at 10 °C/min and the data was normalized to a 1 mg sample mass.

Dynamic mechanical analysis was carried out on a Seiko model 210 operating in the tensile mode. Samples measuring ca. 15 x 4 x 1.2 mm^3 were cut from the plaques and heated at a rate of 2.0 °C/min from –120 °C to 200 °C. The storage modulus and Tanδ data was collected at a frequency of 1 Hz and the grip to grip distance was set at 10 mm.

Swelling experiments were carried out to determine the relative extent of cross-linking as a function of LiCl content. Samples weighing approximately 100-200 mg were completely immersed in ca. 100 ml dimethyl-formamide (DMF) at ambient conditions. The DMF uptake was measured at their equilibrium swelling level, which was achieved in ca. 10-12 h. To reinforce the swelling results via a sol percentage analysis, the DMF swollen samples were placed in an oven at 65°C for 24 h and weighed. The level of weight loss via this extraction process represents the sol fraction where as the extracted matrix represents the gel fraction.

Mechanical and viscoelastic properties were investigated using stress-strain and stress-relaxation experiments. Dumbbell shaped samples with a gauge length of 18 mm were punched from the plaques for the experiments. The experiments were performed on an Instron model 4400R equipped with a 100 kg_f load cell. The modulus of the materials was obtained from the initial slope of the stress-strain data obtained at a crosshead speed of 200 mm/min. Average

modulus values, based on five separate experiments carried out for the same sample will be cited in this report. For the stress relaxation experiments, the samples were stretched at 500 mm/min by 3 mm to a percent strain of 16.7 and stress was tracked as a function of time. The stress-relaxation experiment was repeated at least four times for the same sample by cutting out a different dumbbell for each run, and the results were extremely reproducible.

3.4 Results and Discussion

Since a large number of samples were prepared in order to carry out this study, it will not be possible to utilize the results for all the samples investigated by all the characterization techniques. Instead, selected results, which are representative of this study shall be presented.

TEM is a valuable technique to examine urea aggregates and their level of dispersion, as demonstrated in several studies [2,3,16]. TEM images for the plaques where only the water content is varied are shown in Fig 3.1. The urea rich aggregates have a higher electron density as compared to the polyol phase and thus appear as darker regions on the micrographs. The contrast in the TEM images is solely due to differences in electron density, and no staining procedure was required to enhance these images. Urea aggregation can be seen even in the plaque with the lowest hard segment content, i.e., P1.0-LC0.0. It is also observed that the urea aggregation distinctly increases as the water content is increased to 2.0, 3.5, and 4.5 pphp. This trend has also been reported in a previous work on actual slabstock PU foams by Armistead et al. [3], although the size of urea aggregates reported in that study was smaller (ca. 300 nm) than that noted here. In the plaque containing 4.5 water pphp (Fig 3.1(d)), urea aggregates of the order of 1 μm can be observed. Since the specimen thickness is of the order of 0.1 μm, these urea aggregates are *not* overestimated in size due to sample thickness effects. It is also pointed out that the samples were stable under the electron beam and there were no signs of beam induced artifacts. In fact, the TEM images were also reinforced using AFM as will be demonstrated in Figs 3.4 and 3.5.

Microphase separation in polyurethane [20,21] and poly(urethane urea) [22] elastomers, as well as in PU foams [3,5,6,16,18] has been extensively studied using SAXS. Unlike microscopy techniques, SAXS does not provide a direct image of the morphology of the material, but indirectly provides structural information at length scales ranging from ca. 10 Å to ca. 500 Å. The SAXS profiles for the series of plaques with varying LiCl content and containing the lowest and highest water content (i.e., 2.0 and 4.5 water pphp) are shown in Fig 3.2, where

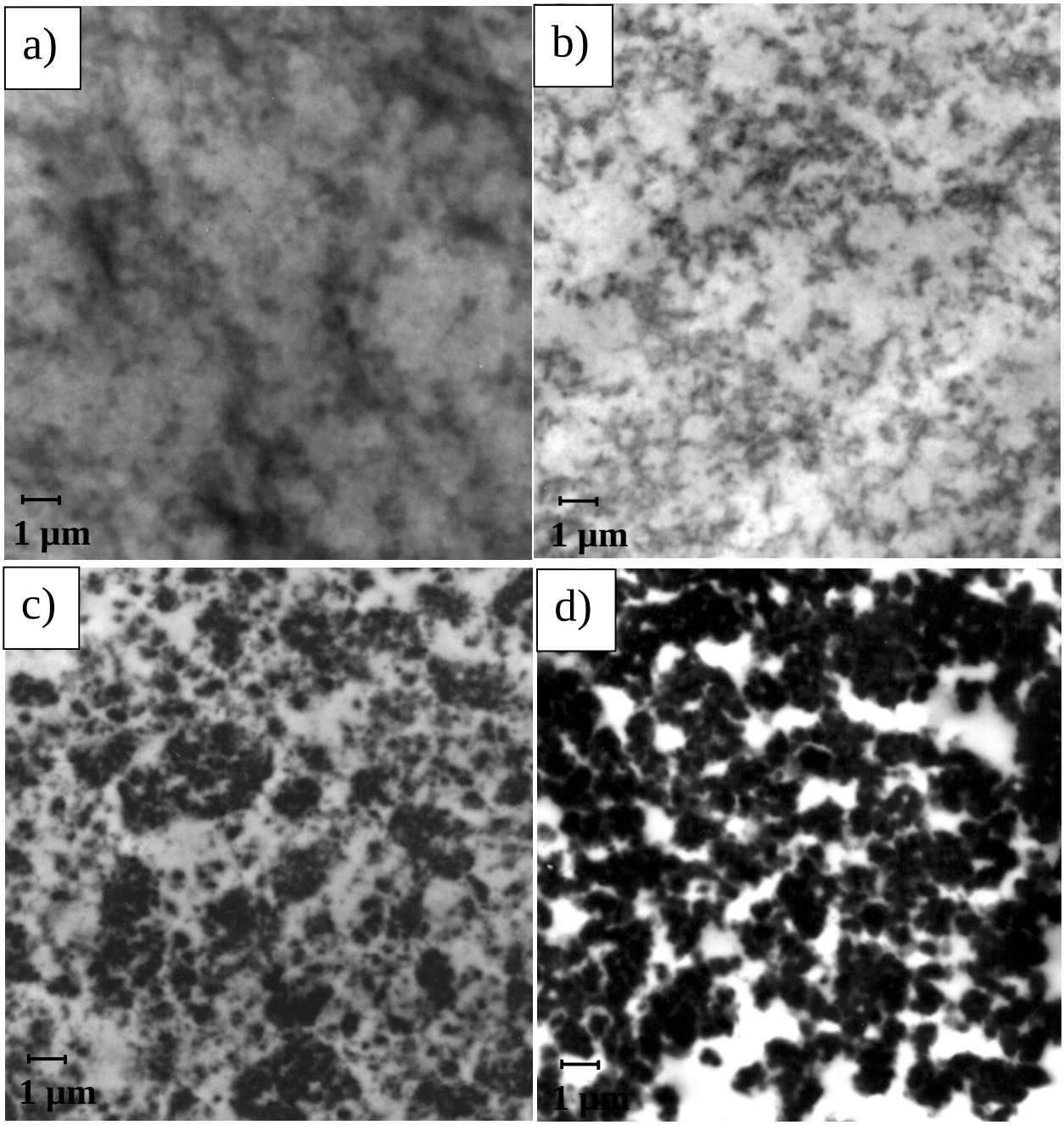

Figure 3.1 Transmission electron micrographs of plaques with varying water content: a) P1.0-LC0.0, b) P2.0-LC0.0, c) P3.5-LC0.0, and d) P4.5-LC0.0

normalized smeared scattered intensity is plotted as a function of the scattering vector 's'. The scattering vector is defined as $s = (2/\lambda)\sin(\theta/2)$ where λ is the wavelength and θ is the radial scattering angle. The presence of a first order interference which appears as a shoulder in all the plaques at ca. 0.01 $Å^{-1}$ indicates that all plaques are microphase separated with an average interdomain spacing of ca. 100 Å, in conformity with previously reported results on related systems [3,16,18].

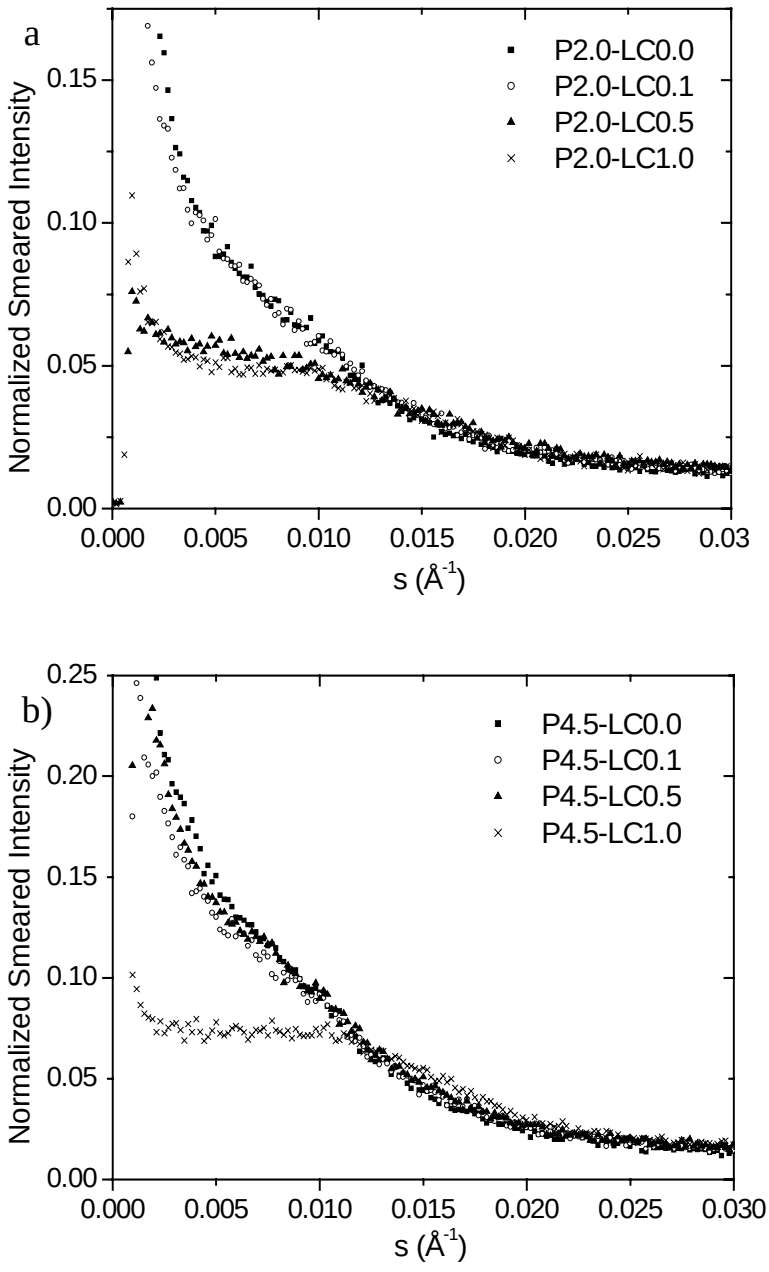

Figure 3.2 Small angle x-ray scattering profiles: a) 2.0 water pphp series with varied LiCl content, b) 4.5 water pphp series with varied LiCl content

Fig 3.2(a) presents the effect of incorporating LiCl in plaque formulations for low water contents (2.0 water pphp). It is seen that incorporating 0.1 LiCl pphp does not result in any drastic changes, at least as revealed by SAXS. However, samples P2.0-LC0.5 and P2.0-LC1.0 display marked differences as compared to P2.0-LC0.0. In both of these materials, the scattering intensity at low 's' values ($s < 0.005$ $Å^{-1}$) is lower than that exhibited by P2.0-LC0.0. Since larger morphological features contribute to the low angle scattering intensity, the SAXS curves strongly suggest that incorporation of LiCl reduces the formation of the urea aggregates. This observation will be further supported by TEM and AFM. Fig 3.2(a) also reveals that there is a considerable sharpening of the SAXS shoulder in samples P2.0-LC0.5 and P2.0-LC1.0. This further suggests that in LiCl containing samples, the urea microdomains are more uniformly distributed in the polyol matrix and that the formation of urea aggregates is minimized.

Fig 3.2(b) presents the SAXS results for the series containing the highest water content of 4.5 water pphp. It is noted that the SAXS profiles are relatively similar for samples P4.5-LC0.0, P4.5-LC0.1, and P4.5-LC0.5. However, the observation that the SAXS curves remain relatively unaltered is not conclusive evidence that the morphological features of these materials are similar, as will be noted later from microscopy results. The SAXS curve of P4.5-LC1.0 displays a significantly sharper shoulder and a reduced scattering intensity at low angles. This observation suggests that when the hard segment content is higher (for example, as compared to the 2.0 water pphp series), it takes a relatively higher dose of LiCl to lead to a considerable reduction of the urea rich regions which contribute to the scattering intensity at low angles.

The TEM images for plaques P2.0-LC0.0 and P2.0-LC0.1 are presented in Fig 3.3. Urea aggregates ca. 0.1 – 0.3 μm in size are observed in plaque P2.0-LC0.0 where as this aggregation

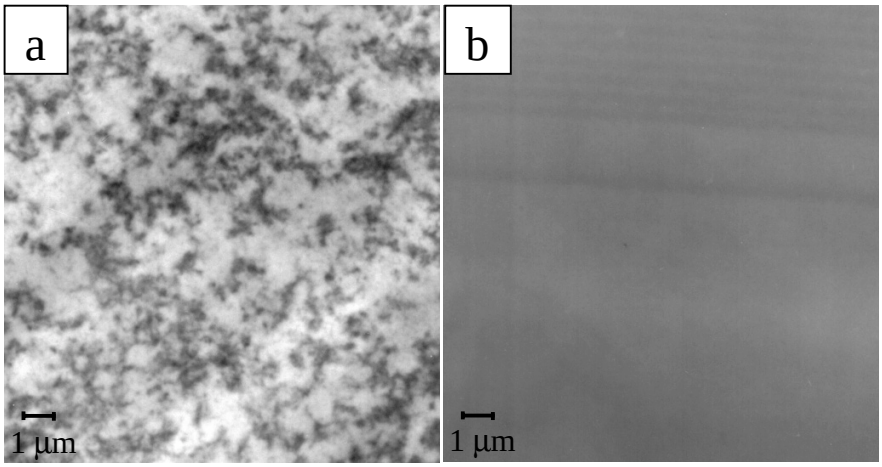

Figure 3.3 Transmission electron micrographs of plaques: a) P2.0-LC0.0 and b) P2.0-LC0.1

is absent in P2.0-LC0.1. Clearly, addition of even a small amount of LiCl in this case was enough to prevent the formation of the urea aggregates. The reader needs to be reminded however that plaque P2.0-LC0.1 is microphase separated, as was proved via SAXS. Thus the incorporation of LiCl even at a level of 0.1 pphp led to the urea microdomains becoming more uniformly distributed in the soft polyol phase. Samples P2.0-LC0.5 and P2.0-LC1.0, which are also microphase separated (as shown by SAXS), also did not show any signs of urea aggregation via TEM and are thus not presented here.

TEM images for the 3.5 water pphp series with varying LiCl content are shown in Fig 3.4. It can be seen that P3.5-LC0.0 displays urea aggregates with sizes of ca. 0.2 – 0.6 μm. In sample P3.5-LC0.1, the urea aggregates are observable but are found to be irregularly dispersed in the polyol phase. Plaques P3.5-LC0.5 and P3.5-LC1.0 do not show signs of any urea aggregation behavior via TEM. These micrographs clearly suggest that addition of LiCl systematically leads to a reduction of the *macro*-connectivity of the urea aggregates. The parallel sets of lines observed in Figs 3.4(b) and 3.4(d) are 'chatter' marks due to the cryo-microtomy, and are not representative of sample morphology. The TEM results for the 4.5 water pphp series (not presented in this report), led to a similar reduction in the urea aggregation on LiCl addition.

AFM has been discussed as an important technique to examine the microphase separation in flexible PU foam systems [9,16]. It has been demonstrated that AFM images, in general, support the TEM images, and can also provide valuable information on the phase-separation behavior when the urea microdomains do not show any aggregation, but are scattered more uniformly in the polyol phase [16]. A set of AFM images for the 3.5 water pphp series with varying LiCl content are presented in Fig 3.5. In AFM phase-imaging, a higher modulus material typically induces a higher phase offset and appears lighter in color as opposed to a softer phase which appears darker. Thus, for the polyurethanes imaged here, the urea rich regions appear lighter where as darker regions correspond to the softer polyol phase. In general, these images are in excellent agreement with TEM images for the 3.5 water pphp series discussed previously in Fig 3.4. In addition, AFM images of P3.5-LC0.0 and P3.5-LC0.1 indicate that the urea aggregates are not purely based on urea, but have some softer polyol phase residing in them, as has been suggested using x-ray microscopy [4,23]. On addition of LiCl, the urea rich regions are found to be systematically reduced with increasing LiCl content. Examining the AFM images of samples P3.5-LC0.5 and P3.5-LC1.0 shows that there are observable differences in the phase

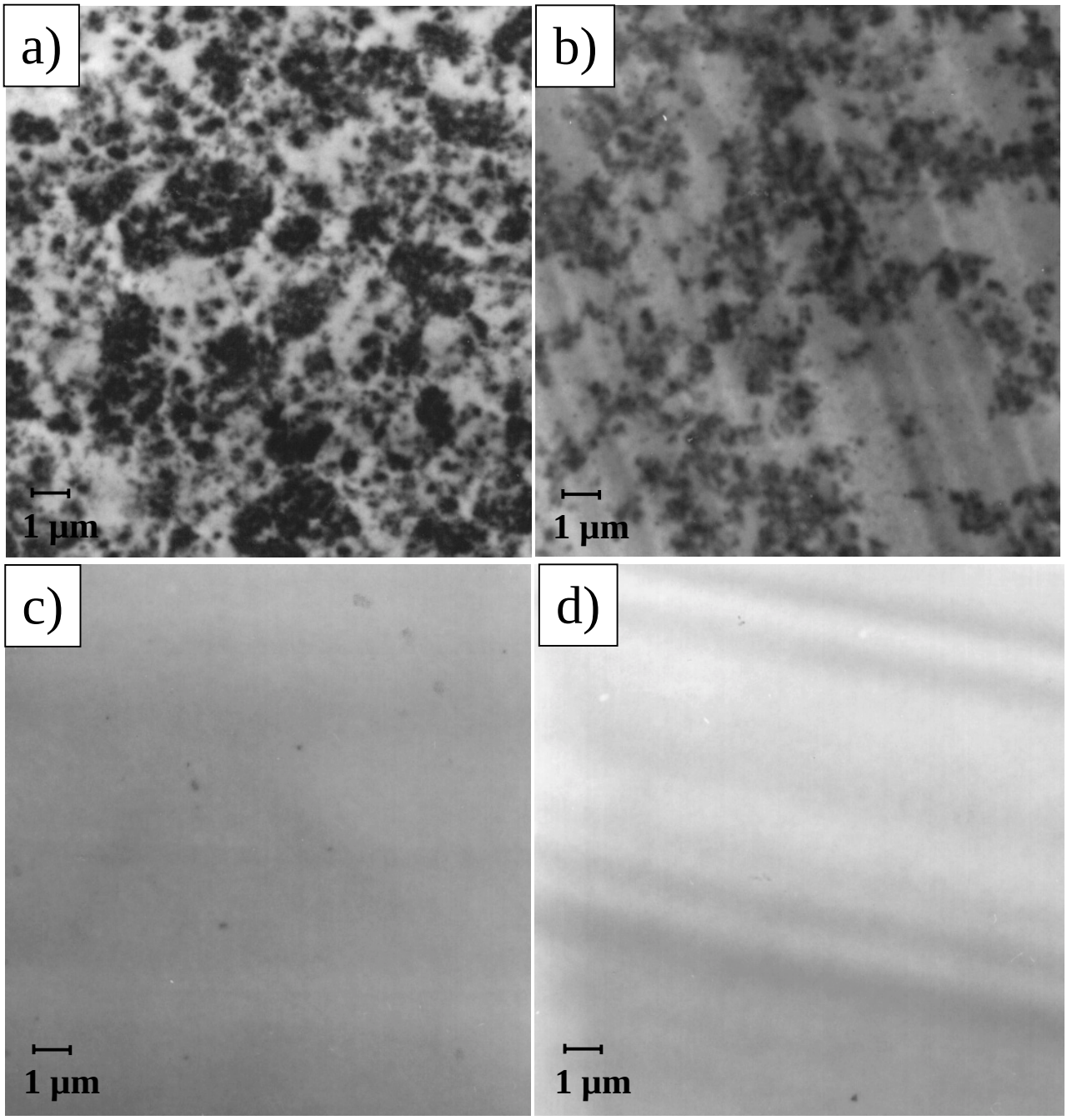

Figure 3.4 Transmission electron micrographs of plaques as a function of LiCl content: a) P3.5-LC0.0, b) P3.5-LC0.1, c) P3.5-LC0.5, and d) P3.5-LC1.0

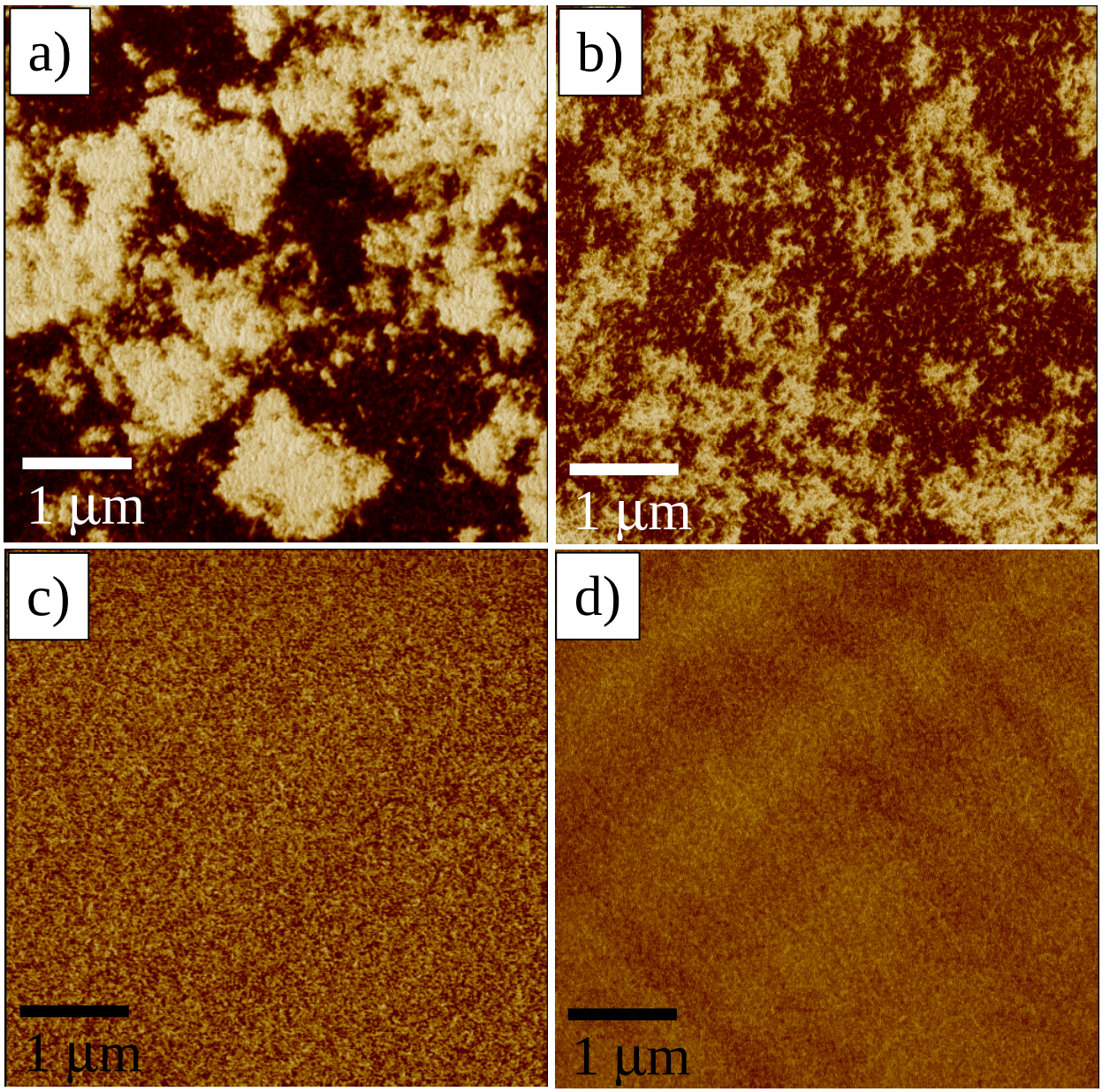

Figure 3.5 Tapping mode atomic force microscopy phase images for samples with varying LiCl content: a) P3.5-LC0.0, b) P3.5-LC0.1, c) P3.5-LC0.5, and d) P3.5-LC1.0

separation behavior even at this scale-length. The size of the urea rich regions appears to be somewhat bigger in sample P3.5-LC0.5 and also shows greater phase contrast between the hard and the soft phase as compared to plaque P3.5-LC1.0. The AFM images for the other two series investigated (not presented in this report) also show similar trends.

WAXS was used to probe the *micro*-connectivity, or the regularity in segmental packing of the plaques investigated. As shown in Fig 3.6, a weak but distinct diffraction peak corresponding to a d-spacing of 4.7 Å spacing is present in P4.5-LC0.0 where as this peak is found to be absent in P4.5-LC1.0. Plaques with intermediate LiCl content show a systematic loss in the peak intensity as LiCl content is increased and are thus not presented. Although the exact source of this reflection has not been completely identified, workers have postulated this local

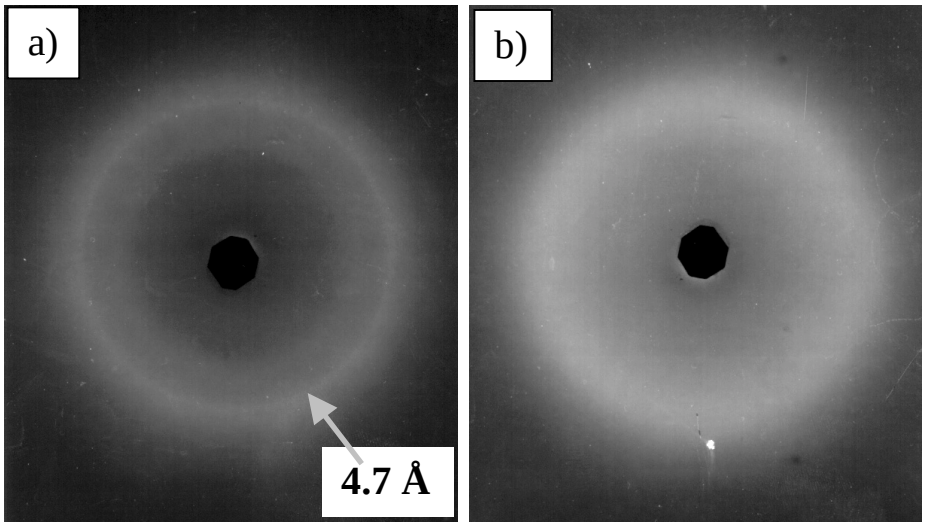

Figure 3.6 Wide angle x-ray scattering patterns for plaques: a) P4.5-LC0.0 and b) P4.5-LC1.0

ordering to be due to the existence of inter-segmental bidentate hydrogen bonding [16]. The WAXS patterns thus suggest that addition of LiCl not only leads to a reduction in connectivity at the urea aggregate level, but also reduces the *micro*-connectivity or the regularity in packing order between the hard segments, thereby leading to reduced cohesiveness between the hard segments. This observation was found to hold for the 2.0 and 3.5 water pphp series as well.

Since LiCl is known to alter reactivity paths by partially blocking the amine catalyst which catalyzes the 'blow' reaction [24], it was essential to compare the quality of network build-up in plaques with and without LiCl. The results from swelling and sol % analyses for the three different series investigated are presented in Table 3.2 and Fig 3.7 respectively. From Table

3.2, it is seen that the addition of LiCl did not cause drastic changes in the quality of the network, which is reflected by the equilibrium swelling level of the different plaques. The equilibrium

Sample	Equilibrium Swelling Ratio [DMF Uptake (g) / Sample Weight (g)]
P2.0-LC0.0	3.8
P2.0-LC0.1	1.8
P2.0-LC0.5	1.8
P2.0-LC1.0	2.3
P3.5-LC0.0	2.9
P3.5-LC0.1	2.3
P3.5-LC0.5	2.1
P3.5-LC1.0	2.2
P4.5-LC0.0	4.0
P4.5-LC0.1	2.1
P4.5-LC0.5	2.0
P4.5-LC1.0	2.5

Table 3.2 – Equilibrium swelling ratio as a function of LiCl content

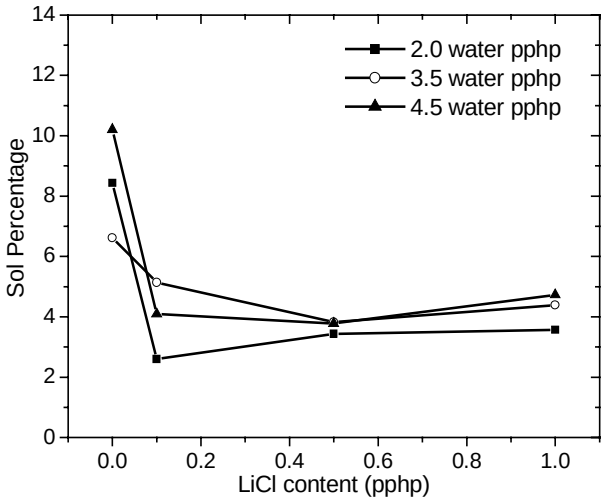

Figure 3.7 Sol% as a function of LiCl content for the 2.0, 3.5, and 4.5 water pphp series

swelling content, measured as the weight of the solvent (DMF) uptake, normalized to the initial weight of the sample, for the samples incorporating LiCl is always lower than that of the sample which does not employ the additive. In addition, results from the sol % analyses for all the three series of plaques are plotted in Fig 3.7. In support of the swelling experiments, the sol % for the materials containing no LiCl are found to be always higher than for the formulations containing LiCl. Thus it is concluded that incorporation of LiCl does not inhibit the formation of a covalent network; in fact, these data imply that the addition of LiCl led to a network which had a cross-link density greater than the cross-link density of the same formulation without LiCl.

DSC was utilized to study the effect of LiCl content on the soft-segment glass transition breadth and position. The DSC results for the 4.5 water pphp series are shown in Fig 3.8. All materials display a soft segment glass transition in the range of –55 to –45 °C, in agreement with previously reported values for similar systems [3]. It is observed that there is a small but systematic broadening of the glass transition region on addition of LiCl. It has already been shown using TEM and AFM that addition of LiCl dispersed the urea microdomains in a more

uniform fashion in the polyol matrix. A possible explanation for this broadening in the soft segment glass transition could be that the urea microdomains impose greater mobility restrictions on the soft segment fraction when the LiCl content is increased.

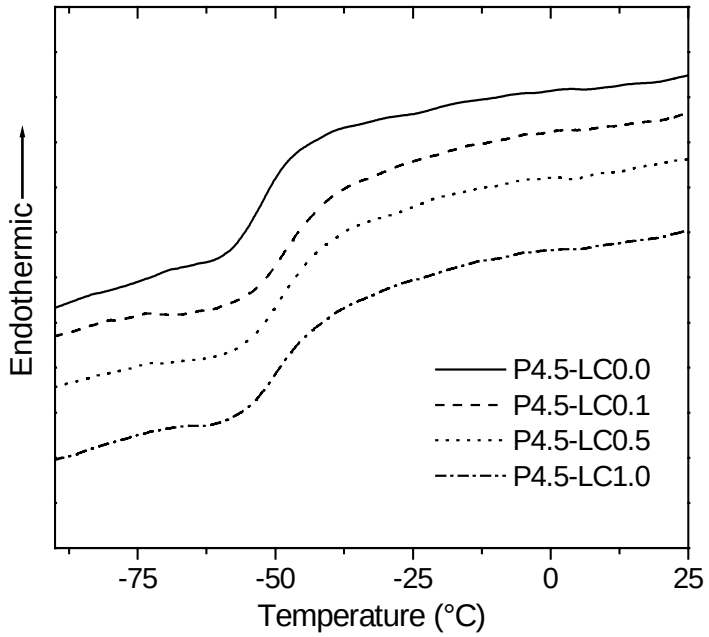

Figure 3.8 Soft segment glass transition observed via DSC as a function of LiCl content

The plaques prepared were also studied using DMA, and results from this analysis are presented in Figs 3.9-3.11. In Fig 3.9, storage moduli and Tanδ are plotted as a function of temperature for the plaques with varied water content and containing no LiCl. The storage modulus curves in Fig 3.9(a) go through a sharp transition from the glassy state to the rubbery state. This is followed by a flat rubbery plateau region extending up to at least 200 °C after which degradation begins. As expected, it is noted that the rubbery modulus systematically increases as the water content is increased, an effect which has been previously noted in slabstock PU foams [3]. Increasing the water content does not greatly influence the soft segment glass transition position, as can be seen in the Tanδ curves in Fig 3.9(b). This observation indirectly indicates that the degree of phase separation is similar in all these materials.

Fig 3.10 presents DMA data for the 3.5 water pphp plaque series with varied LiCl content. Incorporation of LiCl alters the dynamic mechanical behavior in two major ways. Firstly, the addition of LiCl substantially reduces the temperature range of the rubbery modulus regime, i.e., the LiCl containing plaques lose their cohesiveness at higher temperatures, as indicated by a substantial drop in their storage moduli at ca. 125 °C. Secondly, it is seen that

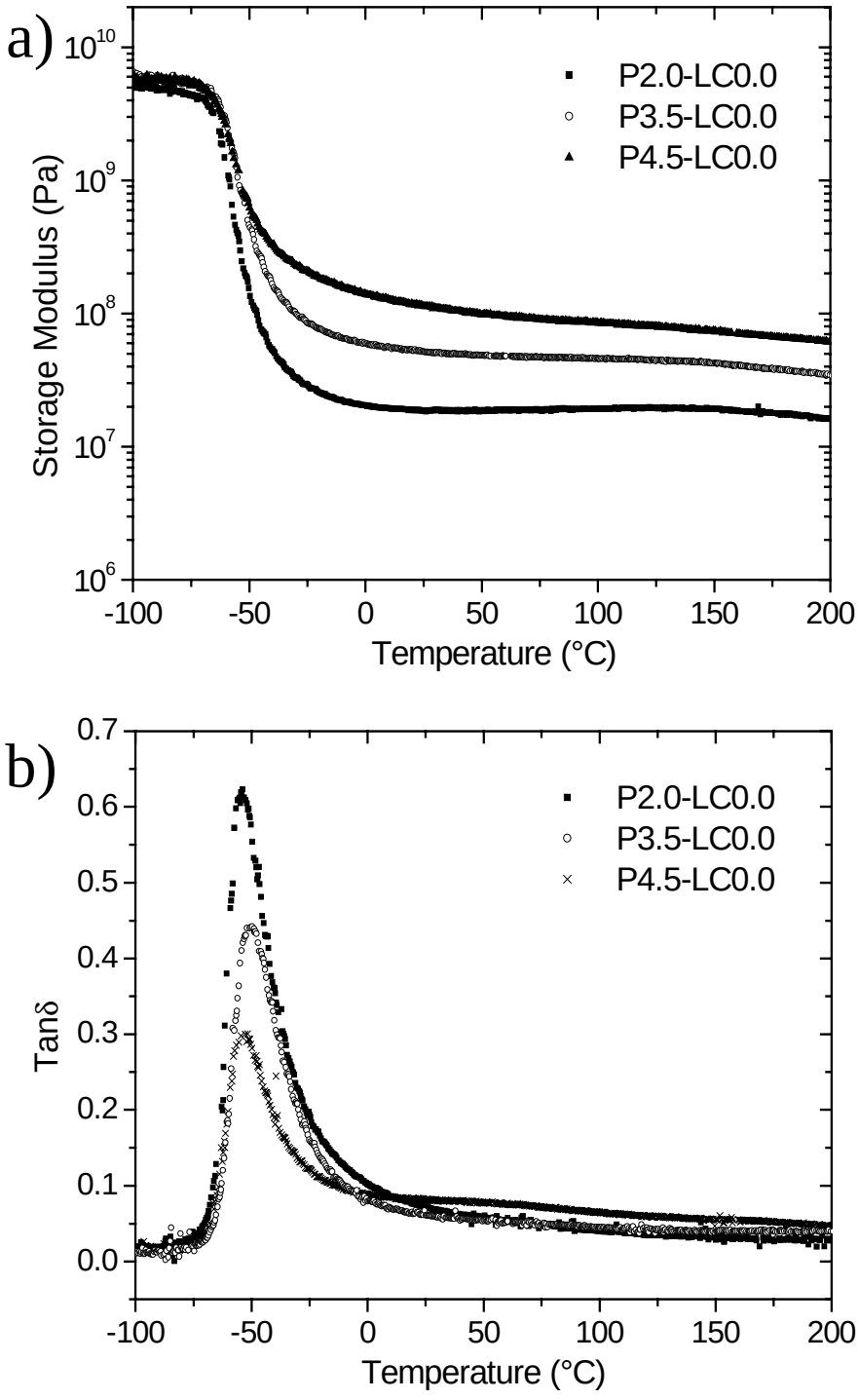

Figure 3.9 Dynamic mechanical analysis results of samples P2.0-LC0.0, P3.5-LC0.0, and P4.5-LC0.0: a) storage modulus, and b) Tanδ

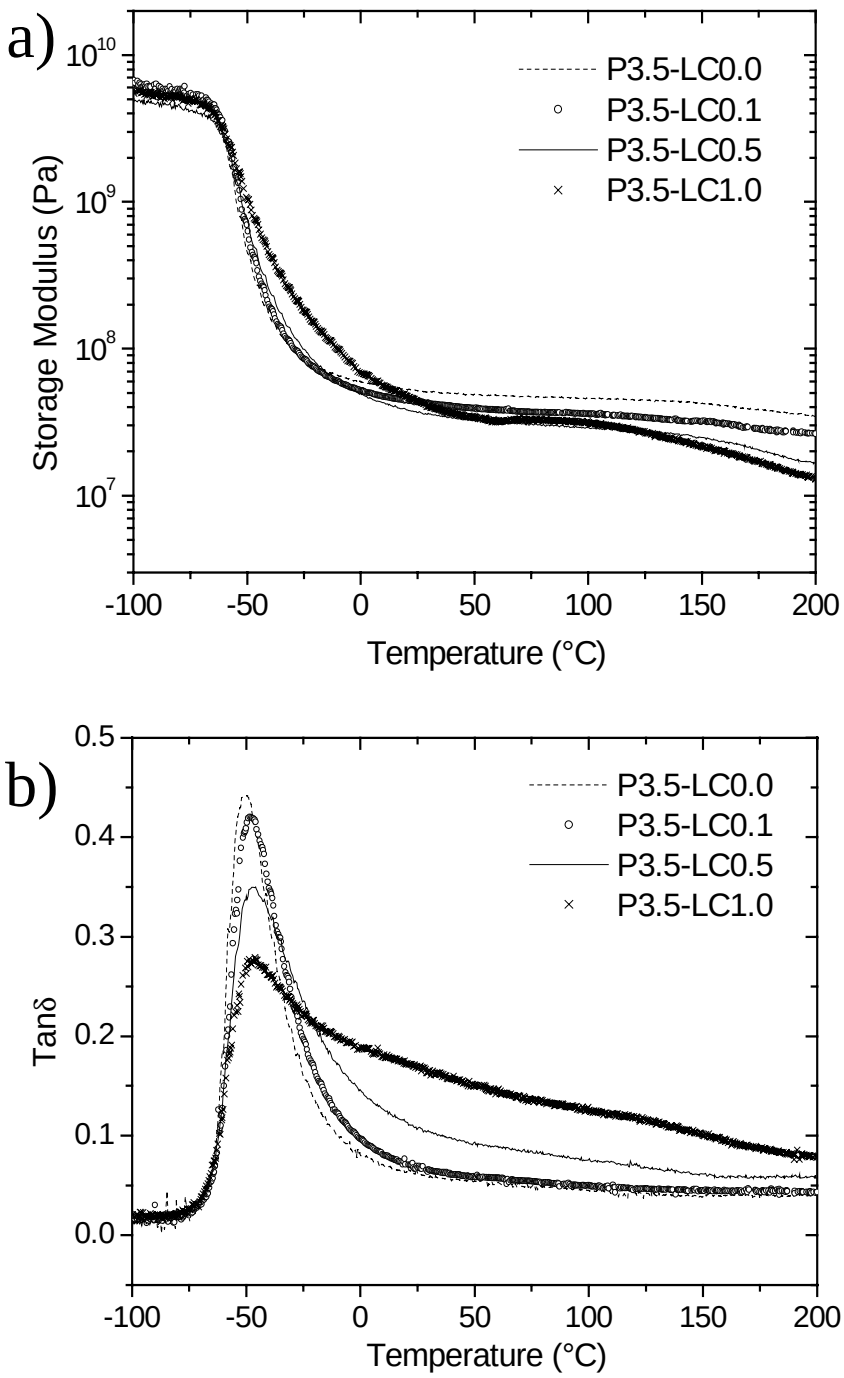

Figure 3.10 Dynamic mechanical analysis results of samples P3.5-LC0.0, P3.5-LC0.1, P3.5-LC0.5, and P3.5-LC1.0: a) storage modulus, and b) Tanδ

addition of LiCl systematically broadens the soft segment glass transition as inferred from storage moduli as well as Tanδ graphs, an effect which was also noted using DSC.

It is seen from Fig 3.11(a) that plaque P4.5-LC0.0 displays a fairly flat extended rubbery plateau up to temperatures approaching ca. 200 °C, which is not observed in the LiCl containing plaques which display a sharp fall in the rubbery modulus at ca. 125 °C. It is suggested that a loss in the *micro* level connectivity, which would promote chain slippage at higher temperatures, might be the cause of this observation. On close inspection of the storage moduli at ca. 25 °C, it is observed that the rubbery modulus for P4.5-LC0.1 and P4.5-LC0.5 is lower than that for P4.5-LC0.0, but for P4.5-LC1.0, the storage modulus is actually greater than that of P4.5-LC0.0. This somewhat surprising behavior was also confirmed using stress-relaxation and modulus experiments (carried out at ca. 25 °C) which are discussed later in this report. It is also noted from both, the storage modulus, and Tanδ curves, that there is a broadening of the glass transition region on addition of LiCl. This supports the DSC data discussed previously, and reinforces the idea that the mobility of a fraction of the soft segment is restricted when the urea microdomains are more uniformly distributed in the soft phase. Also, the soft segment mobility is not affected to the extent that it changes the absolute position of the Tanδ peak, but only leads to T_g broadening effects. The soft segment T_g broadening was very minimal as observed in the 2.0 water pphp series, due to its relatively lower hard segment content.

Stress-relaxation was carried out at ambient conditions and results for the 4.5 water pphp series are presented in Fig 3.12. Recall that the stress-relaxation experiments were carried out at least four times for each sample and led to excellent reproducibility. The stiffness of the materials (as observed from the initial stress level of the stress relaxation curves) is found to first decrease and then interestingly increase as the LiCl content is increased. P4.5-LC0.1 and P4.5-LC0.5 are observed to have a lower stiffness as compared to P4.5-LC0.0. Plaque P4.5-LC1.0, however, displays a higher stiffness as compared to P4.5-LC0.0, in agreement with the room temperature storage modulus data obtained from DMA for this series. In general, the rate of stress decay increases as the LiCl content is increased, in agreement with the findings of Moreland et. al. [18]. The 2.0 and 3.5 water pphp series showed similar trends with regards to initial stress levels, however, for both of these series the 0.0 LiCl pphp sample exhibited the highest initial stress.

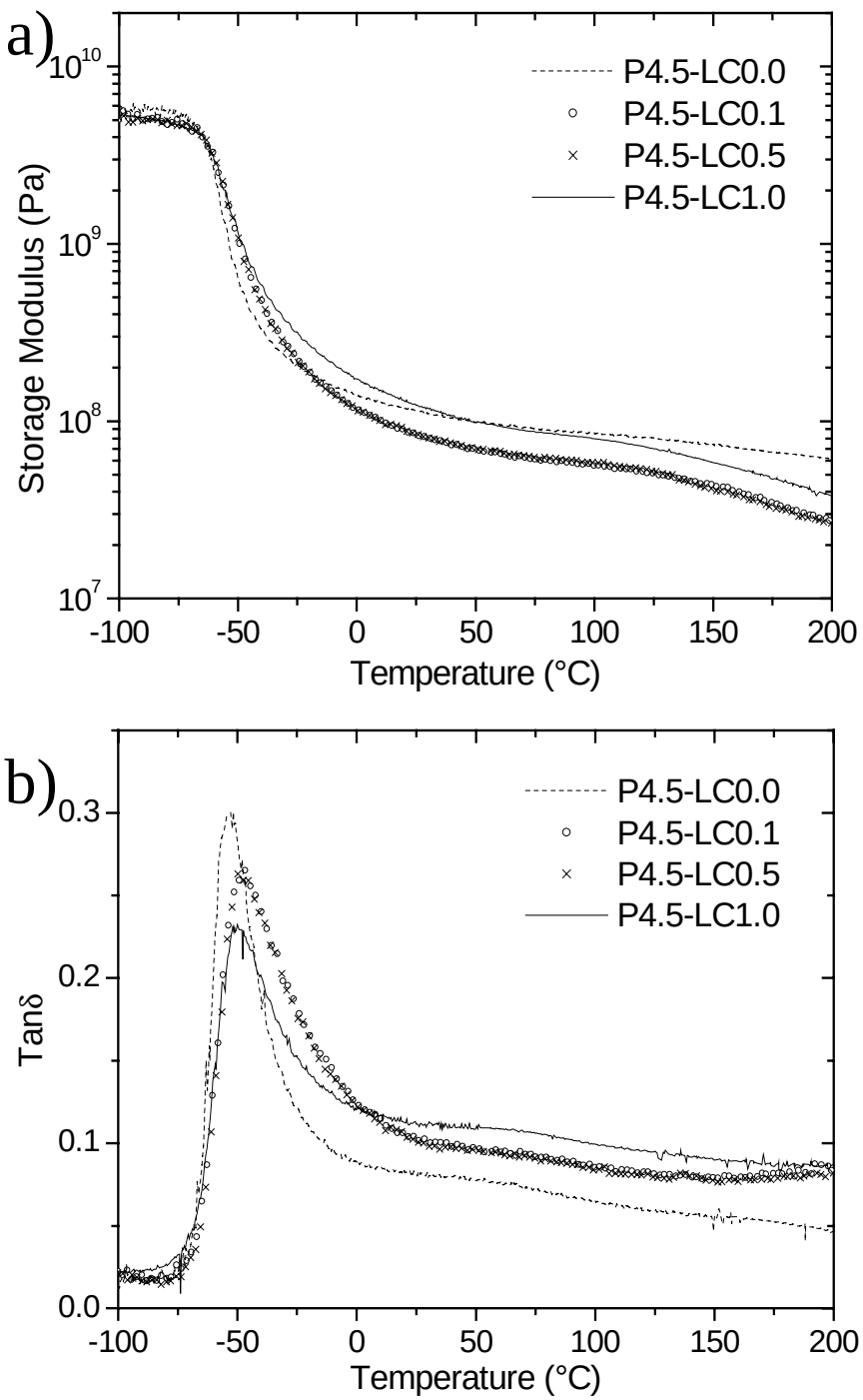

Figure 3.11 Dynamic mechanical analysis results of samples P4.5-LC0.0, P4.5-LC0.1, P4.5-LC0.5, and P4.5-LC1.0: a) storage modulus, and b) Tanδ

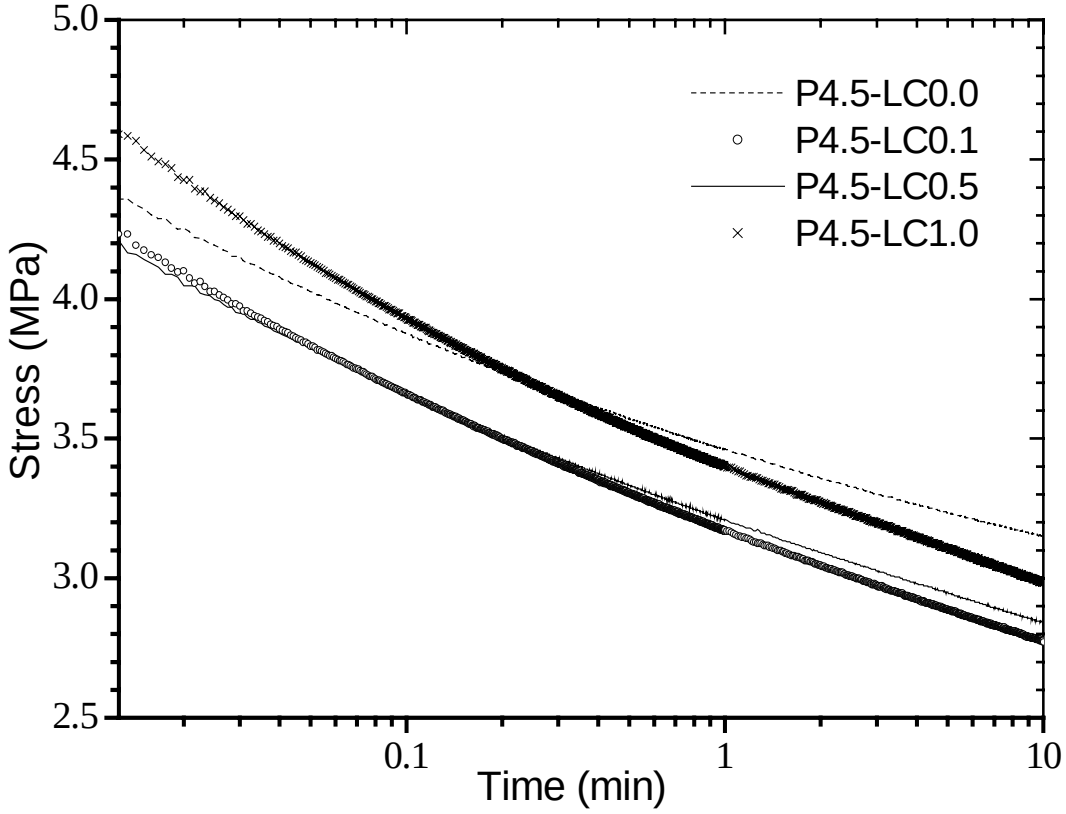

Figure 3.12 Stress-relaxation graphs for the 4.5 water pphp series with varied LiCl contents

Modulus results from the stress-strain analyses carried out at ambient conditions for all three series of plaques analyzed are displayed in Fig 3.13. As expected, the modulus is found to go up as the water content used in the formulation is increased. For example, the average modulus for P2.0-LC0.0, P3.0LC0.0, and P4.5LC0.0 are found to be 5.6, 18.2, and 34.4 MPa respectively.

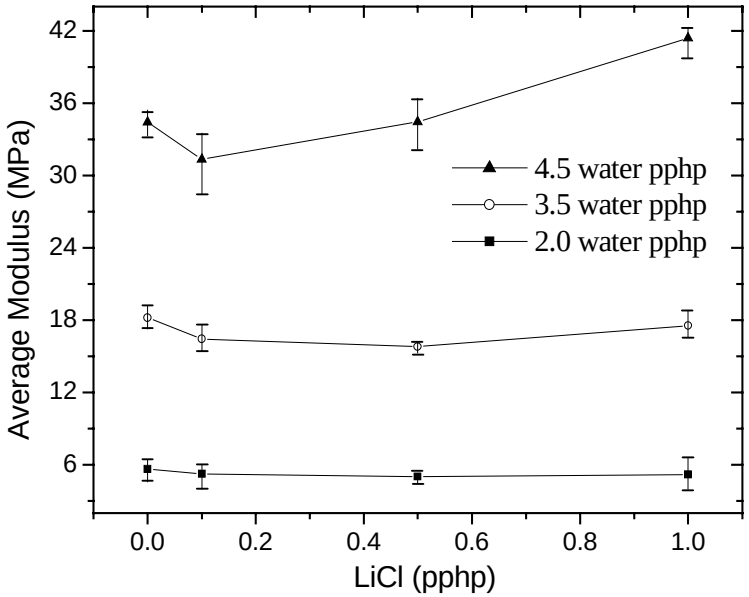

Figure 3.13 Average modulus values as a function of LiCl content for the 2.0, 3.5, and 4.5 water pphp

Inspecting the 2.0 and 3.5 water pphp series suggests that the modulus is not significantly affected by the LiCl content. However, for the 4.5 water pphp series, the modulus first decreases and then increases as the LiCl content is increased. A loss in the *macro* level connectivity is thought to lead to the reduced modulus of P4.5-LC0.0. As the LiCl content is increased, the urea microdomains get more homogeneously distributed in the system (as observed by SAXS, TEM, and AFM) and impose mobility restrictions on the soft segment fraction (as observed by DSC and DMA). This leads to P4.5-LC1.0 possessing a modulus greater than that of P4.5-LC0.0. The modulus of the 2.0 and 3.5 water pphp series plaques with and without LiCl remained relatively unaffected due to their lower hard segment contents.

3.5 Conclusions

Lithium chloride is used as a probe to examine urea phase connectivity and its effect on mechanical and viscoelastic properties of plaques based on slabstock flexible PU foam formulations. Urea phase connectivity is present at different length-scales and is assessed using

multiple characterization techniques. The issue of *macro* level connectivity, or the physical associations between the large scale urea aggregates, is addressed using SAXS, TEM, and AFM. The level of urea aggregation is noted to increase with the water content (or hard segment content). Lithium chloride, when added to the plaque formulations, is observed to reduce the *macro* connectivity of the urea phase. The loss in urea phase *macro* connectivity leads to a reduction in the modulus of the plaques, as observed at ambient conditions for the low LiCl content samples. At higher LiCl contents, the urea microdomains become more uniformly dispersed in the polyol phase and start imposing greater mobility restrictions on the soft segment fraction. For the high hard segment containing systems, this leads to an observed increase in the room temperature modulus.

Micro connectivity, or the regularity in packing of the urea hard segments, was assessed using WAXS. LiCl was shown to disrupt the ordering of the urea hard segments within the urea microdomains and led to materials which exhibited higher rates of stress-relaxation as compared to their counterparts which did not contain the additive. The loss in *micro* level connectivity also leads to the hard segment domains losing their cohesiveness at higher temperatures, as indicated by their reduced temperature range in the rubbery modulus regime. From a more fundamental point of view, the interaction of LiCl with model urea and urethane compounds will be discussed in Chapter 6.

3.6 References

[1] Hepburn C. Polyurethane Elastomers, 2nd ed.: Elsevier Applied Science, 1991.
[2] Herrington R, Hock K. Flexible polyurethane foams, 2nd ed.: Dow Chemical Co.: Midland, MI, 1998.
[3] Armistead JP, Wilkes GL, Turner RB. J Appl Polym Sci 1988;35:601.
[4] Ade H, Smith AP, Cameron S, Cieslinski R, Mitchell G, Hsiao B, Rightor E. Polymer 1995;36:1843.
[5] Kaushiva BD, Dounis DV, Wilkes GL. J Appl Polym Sci 2000;78:766.
[6] Kaushiva BD, Wilkes GL. J Appl Polym Sci 2000;77:202.
[7] Dounis DV, Wilkes GL. J Appl Polym Sci 1997;65:525.
[8] Zhang XD, Bertsch LM, Macosko CW, House DW, Scott RV, Turner RB. Proceedings of Polyurethanes Expo 1998:275
[9] Kaushiva BD, Wilkes GL. Polymer Commun 2000;41:6981.
[10] Moreland JC, Wilkes GL, Turner RB. J Appl Polym Sci 1994;52:549.
[11] Moreland JC, Wilkes GL, Turner RB. J Appl Polym Sci 1994;52:569.

[12] Dounis DV, Moreland JC, Wilkes GL, Dillard DA, Turner RB. J Appl Polym Sci 1993;50:293.
[13] Gao T. Gaofenzi Tongxun 1984;1:69.
[14] Seymour RW, Cooper SL. Adv Urethane Sci 1974;3:66.
[15] Moreland JC, Wilkes GL, Turner RB. J Appl Polym Sci 1991;43:801.
[16] Kaushiva BD, McCartney SR, Rossmy GR, Wilkes GL. Polymer 2000;41:285.
[17] Yontz J, Hsu SL. Macromolecules 2000;33:8415.
[18] Moreland JC, Wilkes GL, Turner RB, Rightor EG. J Appl Polym Sci 1994;52:1459.
[19] Kaushiva BD. PhD Dissertation, Chapter 8: Virginia Polytechnic Institute and State University 2000.
[20] Neumüller W, Bonart R. J Macromol Sci Phys 1974;B(9)3:447.
[21] Koberstein JT, Stein RS. J Polym Sci Polym Phys 1983;21:1439.
[22] Garrett JT, Runt J, Lin JS. Macromolecules 2000;33:6353.
[23] Rightor EG, Urquhart SG, Hitchcock AP, Ade H, Smith AP, Mitchell GE, Priester RD, Aneja A, Appel G, Wilkes GL, Lidy WE. submitted to *Macromolecules.*
[24] Priester RD. of Dow Chemical Co., personal communication.